

Higher $su(N)$ tensor products

This article has been downloaded from IOPscience. Please scroll down to see the full text article.

2001 J. Phys. A: Math. Gen. 34 7685

(<http://iopscience.iop.org/0305-4470/34/37/318>)

View [the table of contents for this issue](#), or go to the [journal homepage](#) for more

Download details:

IP Address: 171.66.16.98

The article was downloaded on 02/06/2010 at 09:17

Please note that [terms and conditions apply](#).

Higher $su(N)$ tensor products

J Rasmussen and M A Walton

Physics Department, University of Lethbridge, Lethbridge, Alberta, Canada T1K 3M4

E-mail: rasmussj@cs.uleth.ca and walton@uleth.ca

Received 15 March 2001

Published 7 September 2001

Online at stacks.iop.org/JPhysA/34/7685

Abstract

We extend our recent results on ordinary $su(N)$ tensor product multiplicities to higher $su(N)$ tensor products. Particular emphasis is put on four-point couplings where the tensor product of four highest weight modules is considered. The number of times the singlet occurs in the decomposition is the associated multiplicity. In this framework, ordinary tensor products correspond to three-point couplings. As in that case, the four-point multiplicity may be expressed explicitly as a multiple sum measuring the discretized volume of a convex polytope. This description extends to higher-point couplings as well. We also address the problem of determining when a higher-point coupling exists, i.e. when the associated multiplicity is non-vanishing. The solution is a set of inequalities in the Dynkin labels.

PACS numbers: 02.20.Sv, 02.20.-a

1. Introduction

The decomposition of tensor products of simple Lie algebra modules has been studied for a long time now. Many elegant results have been found for the multiplicities of the decompositions, the so-called tensor product multiplicities. However, most results pertain to the decomposition of tensor products of *two* irreducible highest weight modules of a simple Lie algebra:

$$M_\lambda \otimes M_\mu = \bigoplus_v T_{\lambda,\mu}^v M_v. \quad (1)$$

M_λ is the module of highest weight λ , while $T_{\lambda,\mu}^v$ is the tensor product multiplicity. This problem is equivalent to the more symmetric one of determining the multiplicity of the singlet in the decomposition of the *triple* product

$$M_\lambda \otimes M_\mu \otimes M_\nu \supset T_{\lambda,\mu,\nu} M_0. \quad (2)$$

Indeed, if ν^+ denotes the weight conjugate to ν , we have $T_{\lambda,\mu,\nu} = T_{\lambda,\mu}^{\nu^+}$. We will use the shorthand notation $\lambda \otimes \mu \otimes \nu$ to represent the left-hand side of (2), and refer to it as a three-point product.

The objective of this paper is to discuss higher $su(N)$ tensor products (or higher-point $su(N)$ couplings), and provide explicit expressions for the associated multiplicities:

$$M_\lambda \otimes M_\mu \otimes \cdots \otimes M_\sigma \supset T_{\lambda,\mu,\dots,\sigma} M_0. \quad (3)$$

Based on a generalization of the Berenstein–Zelevinsky (BZ) method of triangles [1], we have recently obtained very explicit expressions for $T_{\lambda,\mu,\nu}$. The result is a multiple sum formula measuring the discretized volume of a convex polytope associated with the tensor product [2]. It is this idea which shall be extended here to cover higher-point couplings. The main focus will be on four-point couplings. Our results pertain to the A series, $A_r = su(r+1)$.

We also address the problem of determining when a higher-point coupling exists, i.e. when the associated multiplicity is non-vanishing. The solution is a set of inequalities in the Dynkin labels.

2. Ordinary tensor product multiplicities

To fix notation, we review briefly our main result [2] on the computation of ordinary tensor product multiplicities, i.e. on the evaluation of three-point couplings. We refer to [2] for more details.

An $su(r+1)$ BZ triangle, describing a particular coupling (to the singlet) associated with the triple product $\lambda \otimes \mu \otimes \nu$, is a triangular arrangement of

$$E_r = \frac{3}{2}r(r+1) \quad (4)$$

non-negative integers, denoted entries. The entries are subject to certain constraints: the $3r$ outer constraints and the $2H_r$ hexagon identities, where

$$H_r = \frac{1}{2}r(r-1) \quad (5)$$

is the number of hexagons, see below. The case $su(3)$ provides a simple illustration:

$$\begin{array}{ccccc} & & m_{13} & & \\ & n_{12} & & l_{23} & \\ m_{23} & & m_{12} & & \\ n_{13} & l_{12} & n_{23} & l_{13} & \end{array} \quad (6)$$

According to the outer constraints, these $E_2 = 9$ non-negative integers are related to the Dynkin labels of the three integrable highest weights by

$$\begin{array}{lll} m_{13} + n_{12} = \lambda_1 & n_{13} + l_{12} = \mu_1 & l_{13} + m_{12} = \nu_1 \\ m_{23} + n_{13} = \lambda_2 & n_{23} + l_{13} = \mu_2 & l_{23} + m_{13} = \nu_2. \end{array} \quad (7)$$

The entries further satisfy the hexagon conditions

$$n_{12} + m_{23} = n_{23} + m_{12} \quad m_{12} + l_{23} = m_{23} + l_{12} \quad l_{12} + n_{23} = l_{23} + n_{12} \quad (8)$$

of which only two are independent. The number of BZ triangles is the triple tensor product multiplicity $T_{\lambda,\mu,\nu}$.

The generalization of the BZ triangles we consider is obtained by weakening the constraint that all entries are *non-negative* integers to *arbitrary* integers, negative as well as non-negative. The hexagon identities and the outer constraints are still enforced. A triangle will be called a *true* BZ triangle if all its entries are non-negative.

A generalized $su(r+1)$ BZ triangle is built out of H_r hexagons and three corner points. Each hexagon corresponds to two independent constraints on the entries. This leaves

$$E_r - (2H_r + 3r) = H_r \quad (9)$$

that these inequalities define a convex polytope embedded in \mathbb{R}^{H_r} , whose discretized volume is the tensor product multiplicity $T_{\lambda,\mu,\nu}$. As discussed in [2], this volume may be measured explicitly and calculated by a multiple sum:

$$T_{\lambda,\mu,\nu} = \left(\sum_{v_{1,1}} \right) \left(\sum_{v_{2,1}} \sum_{v_{1,2}} \right) \cdots \left(\sum_{v_{r-2,1}} \cdots \sum_{v_{1,r-2}} \right) \left(\sum_{v_{r-1,1}} \cdots \sum_{v_{1,r-1}} \right) 1. \tag{19}$$

Here the summation variables are bounded according to

$$\begin{aligned} & \max\{-N_1, v_{1,r-2}, -N'_2 + v_{2,r-2}, -\mu_{r-2} + v_{1,r-2} - v_{2,r-3} + v_{2,r-2}\} \\ & \leq v_{1,r-1} \leq \min\{n_1, \mu_{r-1} + v_{1,r-2}, \lambda_r - v_{1,r-2} + v_{2,r-2}, \\ & \quad n_2 + v_{1,r-2} - v_{2,r-2}, N'_1, N_2 + v_{2,r-2}\} \\ & \max\{v_{l-1,r-l} - v_{l-1,r-l-1} + v_{l,r-l-1}, -N'_{l+1} + v_{l+1,r-l-1}, \\ & \quad -\mu_{r-l-1} + v_{l+1,r-l-1} - (1 - \delta_{l,r-2})v_{l+1,r-l-2} + v_{l,r-l-1}\} \\ & \leq v_{l,r-l} \leq \min\{\lambda_{r-l+1} - v_{l,r-l-1} + v_{l-1,r-l} + v_{l+1,r-l-1}, \\ & \quad n_{l+1} + v_{l,r-l-1} - v_{l+1,r-l-1}, N_{l+1} + v_{l+1,r-l-1}\} \quad \text{for } 2 \leq l \leq r-2 \\ & \max\{v_{r-2,1}, -N'_r\} \leq v_{r-1,1} \leq \min\{\lambda_2 + v_{r-2,1}, n_r, N_r\} \\ & \max\{v_{1,j-1}, -\mu_{j-1} + v_{1,j-1} + v_{2,j-1} - (1 - \delta_{j,2})v_{2,j-2}\} \\ & \leq v_{1,j} \leq \min\{\mu_j + v_{1,j-1}, \lambda_r - v_{1,j-1} + v_{2,j-1}\} \quad \text{for } 2 \leq j \leq r-2 \\ & \max\{v_{i,j-1} + v_{i-1,j} - v_{i-1,j-1}, -\mu_{j-1} + v_{i,j-1} + v_{i+1,j-1} - (1 - \delta_{j,2})v_{i+1,j-2}\} \\ & \leq v_{i,j} \leq \lambda_{r-i+1} - v_{i,j-1} + v_{i+1,j-1} + v_{i-1,j} \quad \text{for } 2 \leq i, j, i+j \leq r-1 \\ & v_{i-1,1} \leq v_{i,1} \leq \lambda_{r-i+1} + v_{i-1,1} \quad \text{for } 2 \leq i \leq r-2 \\ & 0 \leq v_{1,1} \leq \min\{\mu_1, \lambda_r\}. \end{aligned} \tag{20}$$

Due to the freedom in choosing the initial triangle, this is just one out of an infinite class of multiple sum representations of $T_{\lambda,\mu,\nu}$. Its asymmetry in the weights merely reflects the symmetry-breaking choice of initial triangle, and the choice of an order of summation.

3. Four-point products

We focus first on four-point products:

$$M_\lambda \otimes M_\mu \otimes M_\nu \otimes M_\sigma \supset T_{\lambda,\mu,\nu,\sigma} M_0. \tag{21}$$

The objective is to characterize the multiplicity $T_{\lambda,\mu,\nu,\sigma}$ as the discretized volume of a convex polytope, and then to express the volume explicitly as a multiple sum. Our starting point will be the decomposition

$$T_{\lambda,\mu,\nu,\sigma} = \sum_{\rho} T_{\lambda,\mu,\rho} T_{\rho^+, \nu,\sigma} \tag{22}$$

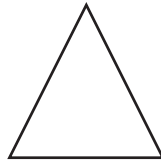
which may be represented graphically by

$$\begin{array}{ccc} \begin{array}{cc} \lambda & \sigma \\ \diagdown & / \\ & \times \\ / & \diagdown \\ \mu & \nu \end{array} & = & \sum_{\rho} \begin{array}{ccc} \lambda & & \sigma \\ & \nearrow & \searrow \\ & \rho & \\ & \nwarrow & \nearrow \\ \mu & & \nu \end{array} \end{array} \tag{23}$$

The arrow indicates that the third weight associated with the coupling involving λ and μ is ρ , while its conjugate, ρ^+ , takes part in the second coupling. Due to the S_4 symmetry of $T_{\lambda,\mu,\nu,\sigma}$ there are many possible decompositions in terms of three-point couplings, associated with different channels. As in the case of the three-point couplings, we are not seeking a symmetric representation of the multiplicity, but merely an explicit multiple sum formula. The decomposition (22) is itself a representation but less explicit than our goal. The former corresponds to considering a sum over products of discretized volumes of convex polytopes embedded in H_r -dimensional Euclidean spaces. The sum is over the r Dynkin labels of the interior weight ρ . Our goal is to represent the multiplicity as the discretized volume of a *single* convex polytope embedded in a $(2H_r + r)$ -dimensional Euclidean space, and eventually to measure explicitly the volume in terms of a multiple sum. The number of parameters is, of course, conserved.

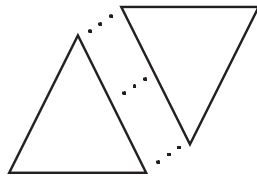
Our approach does not admit an immediate and simple modification in order to obtain a result which is manifestly S_4 symmetric. Taking an average over the possible (symmetry-breaking) channels would provide a straightforward symmetrization but result in a much more complicated expression. One should rather look for an approach which respects the four-coupling nature, and thus does not rely on breaking the coupling up into three-point couplings.

Let



(24)

denote a BZ triangle whose entries have not been specified explicitly. This offers an alternative illustration of the channel (23):



(25)

The dotted lines indicate a gluing of the triangles. These composite objects may be regarded as a generalization of the BZ triangles to diagrams associated with particular choices of four-point channels, governed by a gluing of triangles representing three-point couplings. Disregarding this origin of (25), the configuration is merely an arrangement of $2E_r$ (non-)negative integers subject to certain constraints: $4H_r$ hexagon identities, $4r$ outer constraints representing the four weights and r gluing constraints. Along the dotted lines, the original $2r$ outer constraints are substituted by the r gluing constraints requiring opposite weights to be identical. A four-point diagram is called true if all entries are *non-negative* integers. Explicit examples of four-point diagrams are provided below.

The number of parameters labelling the possible four-point diagrams is

$$2E_r - (4H_r + 4r + r) = 2H_r + r. \quad (26)$$

As in the three-point case, this reflects the existence of $2H_r + r$ basis virtual diagrams that correspond to the basis vectors in the $(2H_r + r)$ -dimensional lattice associated with any given four-point product $\lambda \otimes \mu \otimes \nu \otimes \sigma$. The points in the lattice are the four-point diagrams.

A triangle consisting of zeros alone is called a zero triangle. It is then obvious that $2H_r$ of the basis virtual diagrams are made up of a basis virtual triangle glued together with a

zero triangle, while the remaining r virtual diagrams are associated with the gluing. We shall denote virtual diagrams of the first kind by $\mathcal{V}_{i,j}^{(1)}$ or $\mathcal{V}_{i,j}^{(2)}$ (depending on which triangle includes the non-trivial part)² and call them extended (basis) virtual triangles, and virtual diagrams of the second kind by \mathcal{G}_i and call them ‘simple gluing roots’. It follows from (14) that the latter indeed correspond to pairs of simple roots, as illustrated by this $su(3)$ example (cf (16)):

$$\begin{aligned}
 \mathcal{G}_1 = & \begin{array}{cccc} & & 0 & 0 & 0 & 0 \\ & & \dots & & & \\ & 0 & & \bar{1} & & 0 \\ & & \dots & & & \\ 0 & \bar{1} & \dots & 1 & \bar{1} & \\ & & \dots & & & \\ 0 & & 1 & \dots & 1 & \\ & & & \dots & & \\ 0 & 0 & \bar{1} & 1 & \dots & \end{array} & \mathcal{G}_2 = & \begin{array}{cccc} & & 1 & \bar{1} & 0 & 0 \\ & & \dots & & & \\ & 1 & & 1 & & 0 \\ & & \dots & & & \\ \bar{1} & 1 & \dots & \bar{1} & 0 & \\ & & \dots & & & \\ 0 & & \bar{1} & \dots & 0 & \\ & & & \dots & & \\ 0 & 0 & 0 & 0 & \dots & \end{array}
 \end{aligned} \tag{27}$$

A natural generalization of conventional notation allows us to represent graphically the gluing roots as tree graphs:

$$\begin{aligned}
 \mathcal{G}_1 \sim & \begin{array}{c} 0 \qquad \qquad \qquad 0 \\ \diagdown \qquad \qquad \diagup \\ \qquad \qquad \alpha_1 \qquad \qquad \\ \diagup \qquad \qquad \diagdown \\ 0 \qquad \qquad \qquad 0 \end{array} & \mathcal{G}_2 \sim & \begin{array}{c} 0 \qquad \qquad \qquad 0 \\ \diagdown \qquad \qquad \diagup \\ \qquad \qquad \alpha_2 \qquad \qquad \\ \diagup \qquad \qquad \diagdown \\ 0 \qquad \qquad \qquad 0 \end{array}
 \end{aligned} \tag{28}$$

These graphs, of course, represent couplings that do not exist (i.e. they have vanishing multiplicities) but nevertheless serve to illustrate the power of virtual diagrams. One may even extend the summation range in (23) to include them, since the associated algebraic expressions (22) merely contribute zeros whenever non-true diagrams are encountered.

As in the three-point case, we may now characterize any diagram \mathcal{D} in the lattice by specifying an initial diagram \mathcal{D}_0 :

$$\mathcal{D} = \mathcal{D}_0 + \sum_{a=1,2} \sum_{i,j \geq 1}^{i+j=r} v_{i,j}^{(a)} \mathcal{V}_{i,j}^{(a)} - \sum_{i=1}^r g_i \mathcal{G}_i. \tag{29}$$

$v_{i,j}^{(a)}$ and g_i are integers, named linear coefficients. Note that we have chosen a convention with a minus sign in front of the last sum (29). This reflects the intimate relationship between a simple gluing root and (our convention (11) for) a basis virtual triangle:

$$\begin{aligned}
 -\mathcal{V} = & \begin{array}{cccc} & & \bar{1} & & \\ & & \dots & & \\ & \bar{1} & 1 & 1 & \bar{1} \\ & & \dots & & \\ 1 & & & & 1 \\ & & \dots & & \\ \bar{1} & 1 & 1 & \bar{1} & \\ & & \dots & & \\ & & \bar{1} & & \end{array} & \mathcal{G} = & \begin{array}{cccc} & & \bar{1} & & \\ & & \dots & & \\ & \bar{1} & & 1 & \bar{1} \\ & & \dots & & \\ 1 & & & & 1 \\ & & \dots & & \\ \bar{1} & 1 & \dots & & \bar{1} \\ & & \dots & & \\ & & \bar{1} & & \end{array}
 \end{aligned} \tag{30}$$

One may, of course, choose to substitute the gluing roots with virtual triangles. However, that would introduce redundant parameters that cannot be fixed. This is because such extended gluing roots have the same number of entries as virtual triangles but fewer constraints. $su(2)$

² The lower indices i and j refer to any chosen labelling of the H_r hexagons and, thus, of the associated virtual triangles. (13) is a merely a convenient choice.

offers a simple illustration of that, where the single gluing root is substituted by a single hexagon:



The redundancy occurs since the hexagon identities only allow us to fix a relation between the two extra entries e and e' . This ‘uniformization’ makes possible relations between higher-point $su(N')$ couplings and lower-point $su(N)$ couplings, when N is sufficiently larger than N' . The four-point $su(2)$ diagram above may thus be embedded in a three-point $su(N \geq 4)$ diagram. We hope to discuss such relations in the future. Here, however, we refrain from replacing the gluing roots.

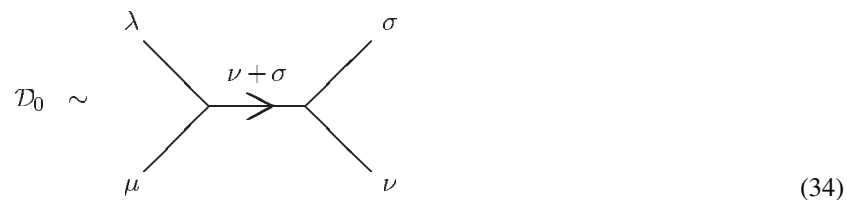
Now we turn to the construction of a convenient initial diagram \mathcal{D}_0 . Referring to (22) we know that

$$\begin{aligned} \rho &= \lambda^+ + \mu^+ - \sum_{i=1}^r n_i^{(1)} \alpha_i & n_i^{(1)} &= (\lambda^+)^i + (\mu^+)^i - \rho^i \in \mathbb{Z}_{\geq} \\ \rho^+ &= \nu^+ + \sigma^+ - \sum_{i=1}^r n_i^{(2)} \alpha_i & n_i^{(2)} &= (\nu^+)^i + (\sigma^+)^i - (\rho^+)^i \in \mathbb{Z}_{\geq}. \end{aligned} \quad (32)$$

It follows that

$$\lambda + \mu + \nu + \sigma = \sum_{i=1}^r m_i \alpha_i \quad m_i \in \mathbb{Z}_{\geq} \quad (33)$$

ensuring the integer nature of the entries. This invites us to choose

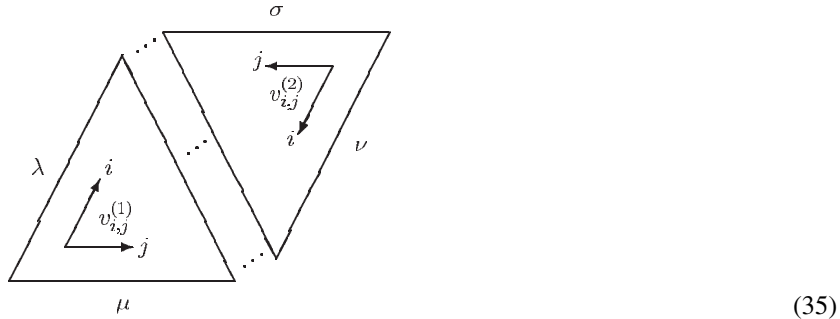


as the initial diagram. This \mathcal{D}_0 is easily constructed explicitly as it corresponds to gluing together our original initial triangles \mathcal{T}_0 (17) associated with the couplings $\lambda \otimes \mu \otimes (\nu + \sigma)$ and $\nu \otimes \sigma \otimes (\nu + \sigma)^+$, respectively.

Now, requiring that \mathcal{D} in (29) is a true diagram leads to a set of inequalities in the linear coefficients v and g . It follows from the structure of the virtual diagrams that this set defines a convex polytope in the Euclidean space $\mathbb{R}^{2H_r+r} = \mathbb{R}^{r^2}$. The discretized volume of the polytope is by construction the tensor product multiplicity $T_{\lambda, \mu, \nu, \sigma}$. This characterization of the four-point tensor product multiplicity is our first main result.

To measure the volume in a straightforward manner, we should organize the inequalities such that a multiple sum expressing the volume may be written down without having to evaluate intersections of polytope faces. This corresponds to choosing an ‘appropriate’ order of summation, as discussed in [2]. Anticipating the extension to higher tensor products to be discussed below, we propose the following procedure.

Let the left (or lower) triangle in (25) correspond initially to the product $\lambda \otimes \mu \otimes (\nu + \sigma)$ such that the right triangle initially corresponds to the product $\nu \otimes \sigma \otimes (\nu + \sigma)^+$. These couplings are of course altered by the gluing process, adding linear combinations of roots to the third weights. Denoting the linear coefficients of the virtual triangles $v_{i,j}^{(1)}$ and $v_{i,j}^{(2)}$, respectively, we may choose the labelling indicated in the following diagram (cf (13)):



An appropriate order of summation is then obtained by starting with the rightmost variable, $v_{1,1}^{(2)}$, and moving systematically towards the left:

$$T_{\lambda,\mu,\nu,\sigma} = \left(\sum_{v_{1,1}^{(1)}} \right) \left(\sum_{v_{2,1}^{(1)}} \sum_{v_{1,2}^{(1)}} \right) \cdots \left(\sum_{v_{r-1,1}^{(1)}} \cdots \sum_{v_{1,r-1}^{(1)}} \right) \left(\sum_{g_r} \cdots \sum_{g_1} \right) \\ \times \left(\sum_{v_{1,r-1}^{(2)}} \cdots \sum_{v_{r-1,1}^{(2)}} \right) \cdots \left(\sum_{v_{1,2}^{(2)}} \sum_{v_{2,1}^{(2)}} \right) \left(\sum_{v_{1,1}^{(2)}} \right) 1. \tag{36}$$

The summation variables are bounded according to

$$\begin{aligned} & \max\{0, -\sigma_2 + v_{1,2}^{(2)}, v_{1,2}^{(2)} - v_{2,2}^{(2)} + v_{2,1}^{(2)}, -\nu_{r-1} + v_{2,1}^{(2)}\} \\ & \leq v_{1,1}^{(2)} \leq \min\{\sigma_1, v_{1,2}^{(2)}, \nu_r - v_{1,2}^{(2)} + v_{2,1}^{(2)}, \sigma_1 + v_{1,2}^{(2)} - v_{2,1}^{(2)}, v_{2,1}^{(2)}, \nu_r\} \\ & \max\{-\sigma_2 + v_{i-1,2}^{(2)} - v_{i-1,3}^{(2)} + v_{i,2}^{(2)}, v_{i,2}^{(2)} - (1 - \delta_{i,r-2})v_{i+1,2}^{(2)} - \delta_{i,r-2}g_2 + v_{i+1,1}^{(2)}, -\nu_{i+1} + v_{i+1,1}^{(2)}\} \\ & \leq v_{i,1}^{(2)} \leq \min\{\nu_{r-i+1} + v_{i-1,2}^{(2)} - v_{i,2}^{(2)} + v_{i+1,1}^{(2)}, \\ & \quad \sigma_1 + v_{i,2}^{(2)} - v_{i+1,1}^{(2)}, v_{i+1,1}^{(2)}\} \quad \text{for } 2 \leq i \leq r-2 \\ & \max\{v_{i+1,j}^{(2)} + v_{i,j+1}^{(2)} - (1 - \delta_{i+j,r-1})v_{i+1,j+1}^{(2)} - \delta_{i+j,r-1}g_{j+1}, \\ & \quad -\sigma_{j+1} + v_{i-1,j+1}^{(2)} - v_{i-1,j+2}^{(2)} + v_{i,j+1}^{(2)}\} \\ & \leq v_{i,j}^{(2)} \leq \nu_{r-i+1} + v_{i-1,j+1}^{(2)} - v_{i,j+1}^{(2)} + v_{i+1,j}^{(2)} \quad \text{for } 2 \leq i, j, i+j \leq r-1 \\ & \max\{-\sigma_{j+1} + v_{1,j+1}^{(2)}, v_{1,j+1}^{(2)} + v_{2,j}^{(2)} - (1 - \delta_{j,r-2})v_{2,j+1}^{(2)} - \delta_{j,r-2}g_{r-1}\} \\ & \leq v_{1,j}^{(2)} \leq \min\{v_{1,j+1}^{(2)}, \nu_r - v_{1,j+1}^{(2)} + v_{2,j}^{(2)}\} \quad \text{for } 2 \leq j \leq r-2 \\ & \max\{-\nu_1 + g_1, -\sigma_2 + v_{r-2,2}^{(2)} + g_2 - g_3\} \\ & \leq v_{r-1,1}^{(2)} \leq \min\{\sigma_1 - g_1 + g_2, \nu_2 + v_{r-2,2}^{(2)} + g_1 - g_2, g_1\} \\ & -\sigma_{l+1} + v_{r-l-1,l+1}^{(2)} + g_{l+1} - g_{l+2} \\ & \leq v_{r-l,l}^{(2)} \leq \nu_{l+1} - v_{r-l-1,l+1}^{(2)} + g_l - g_{l+1} \quad \text{for } 2 \leq l \leq r-2 \\ & -\sigma_r + g_r \leq v_{1,r-1}^{(2)} \leq \min\{g_r, \nu_r + g_{r-1} - g_r\} \end{aligned}$$

$$\begin{aligned}
& \max\{-n_1 + v_{1,r-1}^{(1)}, -N_2 + v_{1,r-1}^{(1)} - v_{2,r-2}^{(1)} + g_2\} \\
& \quad \leq g_1 \leq \min\{N_1 + v_{1,r-1}^{(1)}, N'_1 - v_{1,r-1}^{(1)} + g_2\} \\
& \max\{-n_i + v_{i-1,r-i+1}^{(1)} + v_{i,r-i}^{(1)} - v_{i-1,r-i}^{(1)}, -N_{i+1} + v_{i,r-i}^{(1)} - (1 - \delta_{i,r-1})v_{i+1,r-i-1}^{(1)} + g_{i+1}\} \\
& \quad \leq g_i \leq N'_i + v_{i-1,r-i+1}^{(1)} - v_{i,r-i}^{(1)} + g_{i+1} \quad \text{for } 2 \leq i \leq r-1 \\
& -n_r + v_{r-1,1}^{(1)} \leq g_r \leq N'_r + v_{r-1,1}^{(1)} \\
& \max\{v_{1,j-1}^{(1)}, -\mu_{j-1} + v_{1,j-1}^{(1)} + v_{2,j-1}^{(1)} - (1 - \delta_{j,2})v_{2,j-2}^{(1)}\} \\
& \quad \leq v_{1,j}^{(1)} \leq \min\{\mu_j + v_{1,j-1}^{(1)}, \lambda_r - v_{1,j-1}^{(1)} + v_{2,j-1}^{(1)}\} \quad \text{for } 2 \leq j \leq r-1 \\
& \max\{v_{i,j-1}^{(1)} + v_{i-1,j}^{(1)} - v_{i-1,j-1}^{(1)}, -\mu_{j-1} + v_{i,j-1}^{(1)} + v_{i+1,j-1}^{(1)} - (1 - \delta_{j,2})v_{i+1,j-2}^{(1)}\} \\
& \quad \leq v_{i,j}^{(1)} \leq \lambda_{r-i+1} - v_{i,j-1}^{(1)} + v_{i+1,j-1}^{(1)} + v_{i-1,j}^{(1)} \quad \text{for } 2 \leq i, j, i+j \leq r \\
& v_{i-1,1}^{(1)} \leq v_{i,1}^{(1)} \leq \lambda_{r-i+1} + v_{i-1,1}^{(1)} \quad \text{for } 2 \leq i \leq r-1 \\
& 0 \leq v_{1,1}^{(1)} \leq \min\{\mu_1, \lambda_r\}
\end{aligned} \tag{37}$$

where the parameters n_i , N_i and N'_i are defined as in (18), with v replaced by $v + \sigma$:

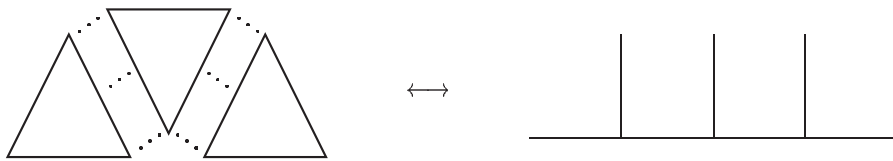
$$\begin{aligned}
n_i &= \lambda^{r-i+1} + \mu^{r-i+1} - (v + \sigma)^i \\
N_i &= (1 - \delta_{i1})n_{i-1} - n_i + \mu_{r-i+1} \\
&= -\lambda^{r-i+1} + (1 - \delta_{i1})\lambda^{r-i+2} - (1 - \delta_{ir})\mu^{r-i} + \mu^{r-i+1} \\
&\quad - (1 - \delta_{i1})(v + \sigma)^{i-1} + (v + \sigma)^i \\
N'_i &= (v + \sigma)_i - N_i \\
&= \lambda^{r-i+1} - (1 - \delta_{i1})\lambda^{r-i+2} + (1 - \delta_{ir})\mu^{r-i} \\
&\quad - \mu^{r-i+1} + (v + \sigma)^i - (1 - \delta_{ir})(v + \sigma)^{i+1}.
\end{aligned} \tag{38}$$

This multiple sum formula is our second main result. For $su(2)$, $su(3)$ and $su(4)$ the explicit multiple sum formulae are provided in section 5.

4. Higher-point couplings

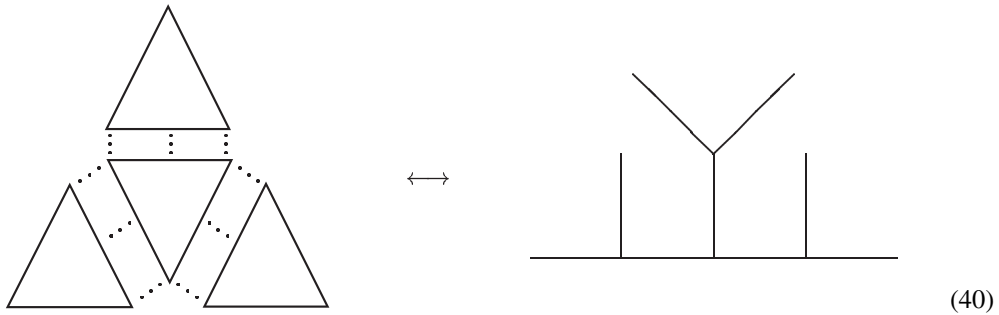
We shall now indicate how one may extend our results on four-point couplings to any higher \mathcal{N} -point coupling, in straightforward fashion.

It is well known that higher-point couplings may be decomposed into three-point couplings along the lines of (22). The various tree-graph channels all have diagram counterparts, as illustrated by the following two examples:

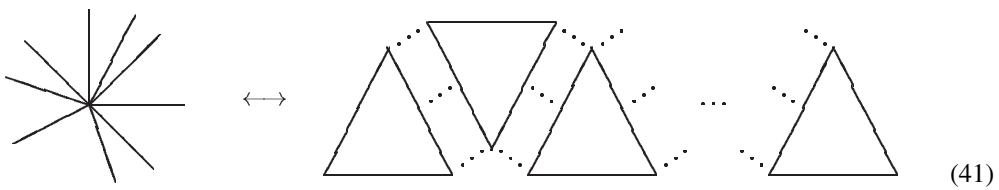


$$\tag{39}$$

and



Since we may choose the channel freely, we can avoid complicated configurations like the ‘rocket’ of (40) and concentrate on the ‘string-like’ ones, like (39) and the following nine-point coupling:



Thus, a \mathcal{N} -point coupling may conveniently be represented by a \mathcal{N} -point diagram consisting of $\mathcal{N} - 2$ triangles glued together along $\mathcal{N} - 3$ pairs of faces to form a string-like configuration. A \mathcal{N} -point diagram is therefore a geometrical arrangement of $(\mathcal{N} - 2)E_r$ (non-)negative integers subject to $2(\mathcal{N} - 2)H_r$ hexagon identities, $\mathcal{N}r$ outer constraints and $(\mathcal{N} - 3)r$ gluing constraints. (This is also true for the more complicated diagrams, such as (40).) This leaves

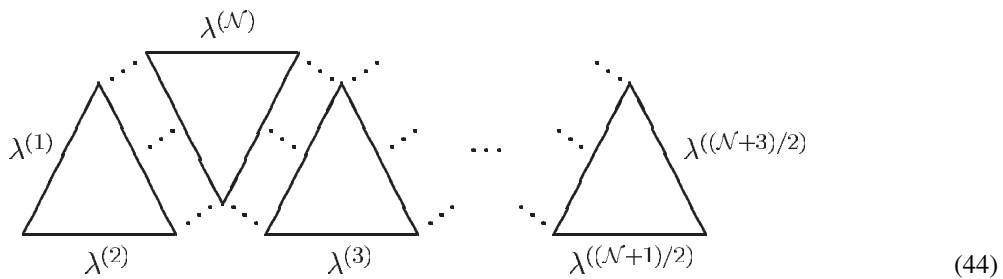
$$(\mathcal{N} - 2)E_r - ((\mathcal{N} - 2)H_r + \mathcal{N}r + (\mathcal{N} - 3)r) = (\mathcal{N} - 2)H_r + (\mathcal{N} - 3)r \quad (42)$$

parameters labelling the possible diagrams. As should be, this is equal to the total number of virtual triangles and simple gluing roots.

Thus, from the point of view of the \mathcal{N} -point diagram, we have two types of virtual diagrams: extended (basis) virtual triangles \mathcal{V} and simple gluing roots \mathcal{G} , exactly as for four-point couplings. The extension of (29) is therefore obvious:

$$\mathcal{D} = \mathcal{D}_0 + \sum_{a=1}^{\mathcal{N}-2} \sum_{i,j \geq 1}^{i+j=r} v_{i,j}^{(a)} \mathcal{V}_{i,j}^{(a)} - \sum_{a=1}^{\mathcal{N}-3} \sum_{i=1}^r g_i^{(a)} \mathcal{G}_i^{(a)}. \quad (43)$$

The initial diagram \mathcal{D}_0 is likewise easy to describe, as it may be constructed by gluing $\mathcal{N} - 2$ initial triangles together. Labelling the \mathcal{N} weights according to (in this example \mathcal{N} is assumed odd)



the participating initial triangles are associated with the couplings

$$\begin{aligned}
 & \lambda^{((\mathcal{N}+1)/2)} \otimes \lambda^{((\mathcal{N}+3)/2)} \otimes (\lambda^{((\mathcal{N}+1)/2)} + \lambda^{((\mathcal{N}+3)/2)})^+ \\
 & (\lambda^{((\mathcal{N}+1)/2)} + \lambda^{((\mathcal{N}+3)/2)}) \otimes \lambda^{((\mathcal{N}+5)/2)} \otimes (\lambda^{((\mathcal{N}+1)/2)} + \lambda^{((\mathcal{N}+3)/2)} + \lambda^{((\mathcal{N}+5)/2)})^+ \\
 & \vdots \\
 & (\lambda^{(3)} + \dots + \lambda^{(\mathcal{N}-1)}) \otimes \lambda^{(\mathcal{N})} \otimes (\lambda^{(3)} + \dots + \lambda^{(\mathcal{N})})^+ \\
 & \lambda^{(1)} \otimes \lambda^{(2)} \otimes (\lambda^{(3)} + \dots + \lambda^{(\mathcal{N})}). \tag{45}
 \end{aligned}$$

The weights are subject to the consistency condition (cf (33))

$$\lambda^{(1)} + \dots + \lambda^{(\mathcal{N})} = \sum_{i=1}^r m_i \alpha_i \quad m_i \in \mathbb{Z}_{\geq}. \tag{46}$$

The characterization of the associated tensor product multiplicity in terms of a convex polytope is materialized by requiring that the diagram should be a true diagram, i.e. all entries must be *non-negative* integers. As before, its discretized volume is the multiplicity by construction. That volume can be expressed explicitly as a multiple sum. An appropriate order of summation is indicated here:

$$T_{\lambda^{(1)}, \lambda^{(2)}, \dots, \lambda^{(\mathcal{N})}} = \left\{ \sum_{v^{(1)}} \right\} \left\{ \sum_{g^{(1)}} \right\} \cdots \left\{ \sum_{v^{(\mathcal{N}-3)}} \right\} \left\{ \sum_{g^{(\mathcal{N}-3)}} \right\} \left\{ \sum_{v^{(\mathcal{N}-2)}} \right\} 1. \tag{47}$$

This generalization of our main results on three- and four-point couplings concludes the extension to general higher-point couplings.

5. Examples and an application

It is of interest to know whether or not a \mathcal{N} -point coupling $\lambda \otimes \mu \otimes \dots \otimes \sigma$ exists, without having to work out the tensor product multiplicity. Based on our multiple sum formulae (36) and (47), one may derive a set of inequalities in the dual and ordinary Dynkin labels of the \mathcal{N} weights, determining when the associated tensor product multiplicity is non-vanishing. The method is an immediate extension of the one employed in [2] when discussing three-point couplings (19). We work out the inequalities for $su(2)$ and $su(3)$ four-point couplings. In principle, it is possible to repeat the procedure for higher rank and higher \mathcal{N} than four, though it rapidly becomes cumbersome.

To the best of our knowledge, similar results only exist for three-point products where, besides our work [2], the works [3, 4] provide recent results and extensive lists of references.

For $su(2)$ the BZ triangle representing the product $\lambda \otimes \mu \otimes \nu$ is unique ($H_1 = 0$):

$$\begin{aligned}
 & \frac{1}{2}(\lambda_1 - \mu_1 + \nu_1) \\
 & \frac{1}{2}(\lambda_1 + \mu_1 - \nu_1) \quad \frac{1}{2}(-\lambda_1 + \mu_1 + \nu_1) \tag{48}
 \end{aligned}$$

Nevertheless, gluing two triangles together leaves one free parameter g . We have

$$\mathcal{D} = \mathcal{D}_0 - g\mathcal{G} \tag{49}$$

where

$$\mathcal{D}_0 = \begin{array}{ccccccc} & & & & \sigma_1 & & 0 \\ & & & & \cdot \cdot \cdot & & \\ & & & & & & \nu_1 \\ & & & & & & \cdot \cdot \cdot \\ \frac{1}{2}(\lambda_1 - \mu_1 + \nu_1 + \sigma_1) & & & & & & \\ & & & & & & \\ \frac{1}{2}(\lambda_1 + \mu_1 - \nu_1 - \sigma_1) & & & & \frac{1}{2}(-\lambda_1 + \mu_1 + \nu_1 + \sigma_1) & & \end{array} \quad (50)$$

and

$$\mathcal{G} = \begin{array}{ccccccc} & & & & 1 & & \bar{1} \\ & & & & \cdot \cdot \cdot & & \\ & & & & & & 1 \\ & & & & & & \cdot \cdot \cdot \\ & & & & \bar{1} & & 1 \end{array} \quad (51)$$

Requiring \mathcal{D} to be a true diagram results in a set of inequalities defining a one-dimensional convex polytope—a line segment. Its discretized volume (or length) is the sought multiplicity:

$$T_{\lambda, \mu, \nu, \sigma} = \sum_{g=\max\{0, S-\lambda_1-\mu_1\}}^{\min\{S-\lambda_1, S-\mu_1, \nu_1, \sigma_1\}} 1 \quad S \equiv \frac{1}{2}(\lambda_1 + \mu_1 + \nu_1 + \sigma_1) \in \mathbb{Z}_{\geq}. \quad (52)$$

The summation, and thus the multiplicity, is non-vanishing if and only if the upper bound is greater than or equal to the lower bound. This requirement defines a four-dimensional cone:

$$0 \leq \lambda_1, \mu_1, \nu_1, \sigma_1, S - \lambda_1, S - \mu_1, S - \nu_1, S - \sigma_1. \quad (53)$$

It is easily verified that (52) and (53) are in accordance with well-known results.

For $su(3)$ the four-point coupling may be characterized by a convex polytope in a four-dimensional Euclidean space. Its discretized volume is the tensor product multiplicity which we find may be expressed as the following multiple sum:

$$T_{\lambda, \mu, \nu, \sigma} = \sum_{v^{(1)}=0}^{\min\{\lambda_2, \mu_1\}} \sum_{g_2=-n_2+v^{(1)}}^{N'_2+v^{(1)}} \sum_{g_1=\max\{-N_2+v^{(1)}+g_2, -n_1+v^{(1)}\}}^{\min\{N_1+v^{(1)}, N'_1+g_2-v^{(1)}\}} \times \sum_{v^{(2)}=\max\{0, -\sigma_2+g_2, -\nu_1+g_1\}}^{\min\{\nu_2, \sigma_1, g_1, g_2, \nu_2+g_1-g_2, \sigma_1-g_1+g_2\}} 1 \quad (54)$$

where the weights are subject to

$$S_i \equiv \lambda^i + \mu^i + \nu^i + \sigma^i \in \mathbb{Z}_{\geq} \quad i = 1, 2 \quad (55)$$

and where

$$\begin{aligned} n_1 &= \lambda^2 + \mu^2 - \nu^1 - \sigma^1 \\ n_2 &= \lambda^1 + \mu^1 - \nu^2 - \sigma^2 \\ N_1 &= -\lambda^2 - \mu^1 + \mu^2 + \nu^1 + \sigma^1 \\ N_2 &= -\lambda^1 + \lambda^2 + \mu^1 - \nu^1 + \nu^2 - \sigma^1 + \sigma^2 \\ N'_1 &= \lambda^2 + \mu^1 - \mu^2 + \nu^1 - \nu^2 + \sigma^1 - \sigma^2 \\ N'_2 &= \lambda^1 - \lambda^2 - \mu^1 + \nu^2 + \sigma^2. \end{aligned} \quad (56)$$

This explicit result is believed to be new.

Analysing when the tensor product multiplicity is non-vanishing leads to the following definition of a cone in the eight-dimensional Dynkin label space:

$$\begin{aligned}
 0 &\leq \lambda_i, \mu_i, v_i, \sigma_i & i = 1, 2 \\
 0 &\leq S_i - \lambda_1 - \lambda_2, S_i - \mu_1 - \mu_2, S_i - v_1 - v_2, S_i - \sigma_1 - \sigma_2 & i = 1, 2 \\
 0 &\leq S_i - \lambda_i - \mu_i, S_i - \lambda_i - v_i, S_i - \lambda_i - \sigma_i \\
 &S_i - \mu_i - v_i, S_i - \mu_i - \sigma_i, S_i - v_i - \sigma_i & i = 1, 2.
 \end{aligned} \tag{57}$$

This explicit characterization is also believed to be new. It is verified immediately that, for one weight equal to zero, (57) reduces to the result for the three-point product discussed in [2], i.e. $T_{\lambda, \mu, v, 0} > 0$ if and only if $T_{\lambda, \mu, v} > 0$.

For ease of use of the formula (36) expressing the tensor product multiplicity $T_{\lambda, \mu, v, \sigma}$ as a multiple sum, we conclude this section by writing down explicitly the result for $su(4)$:

$$\begin{aligned}
 T_{\lambda, \mu, v, \sigma} = & \sum_{v_{1,1}^{(1)}=0}^{\min\{\lambda_3, \mu_1\}} \sum_{v_{2,1}^{(1)}=v_{1,1}^{(1)}}^{\lambda_2+v_{1,1}^{(1)}} \sum_{v_{1,2}^{(1)}=\max\{-\mu_1+v_{2,1}^{(1)}+v_{1,1}^{(1)}, v_{1,1}^{(1)}\}}^{\min\{\lambda_3+v_{2,1}^{(1)}-v_{1,1}^{(1)}, \mu_2+v_{1,1}^{(1)}\}} \sum_{g_3=-n_3+v_{2,1}^{(1)}}^{N'_3+v_{2,1}^{(1)}} \\
 & \times \sum_{g_2=\max\{-N_3+g_3+v_{2,1}^{(1)}, -n_2+v_{1,2}^{(1)}+v_{2,1}^{(1)}-v_{1,1}^{(1)}\}}^{N'_2+g_3+v_{1,2}^{(1)}-v_{2,1}^{(1)}} \sum_{g_1=\max\{-n_1+v_{1,2}^{(1)}, -N_2+g_2+v_{1,2}^{(1)}-v_{2,1}^{(1)}\}}^{\min\{N'_1+g_2-v_{1,2}^{(1)}, N_1+v_{1,2}^{(1)}\}} \\
 & \times \sum_{v_{1,2}^{(2)}=-\sigma_3+g_3}^{\min\{v_3+g_2-g_3, g_3\}} \sum_{v_{2,1}^{(2)}=\max\{-v_1+g_1, -\sigma_2+v_{1,2}^{(2)}+g_2-g_3\}}^{\min\{v_2+v_{1,2}^{(2)}+g_1-g_2, \sigma_1-g_1+g_2, g_1\}} \\
 & \times \sum_{v_{1,1}^{(2)}=\max\{0, -v_2+v_{2,1}^{(2)}, -\sigma_2+v_{1,2}^{(2)}, v_{2,1}^{(2)}+v_{1,2}^{(2)}-g_2\}}^{\min\{v_3, \sigma_1, v_{2,1}^{(2)}, v_{1,2}^{(2)}, v_3+v_{2,1}^{(2)}-v_{1,2}^{(2)}, \sigma_1-v_{2,1}^{(2)}+v_{1,2}^{(2)}\}} 1. \tag{58}
 \end{aligned}$$

The parameters n_i , N_i and N'_i are defined in (38), while the weights are subject to the condition

$$\lambda^i + \mu^i + v^i + \sigma^i \in \mathbb{Z}_{\geq} \quad i = 1, 2, 3. \tag{59}$$

6. Conclusion

We have generalized our recent work on three-point products [2] to cover general \mathcal{N} -point products. That is, we have characterized the associated higher tensor product multiplicities by certain convex polytopes, and measured explicitly their discretized volumes. The latter are the multiplicities and are expressed as multiple sums.

The characterization of the multiplicity as the number of integer points in a convex polytope is an example of a polyhedral combinatorial expression. Alternative polyhedral combinatorial expressions for three-point products (including other simple Lie algebras as well) may be found in [5, 6]. To the best of our knowledge, our result for higher-point products is the first of its kind.

As an application we have also addressed the problem of determining when a tensor product multiplicity is non-vanishing and, as an illustration of the general resolution, provided explicit characterizations for $su(2)$ and $su(3)$. The result for $su(3)$ is believed to be new.

We are currently extending our work (presented here and in [2]) on tensor product multiplicities to fusion multiplicities. The latter are relevant to the representation theory of affine extensions of the Lie algebra, the so-called affine Kac–Moody algebras. They have found prominent applications to conformal field theory with affine Lie group symmetry, the so-called

Wess–Zumino–Witten (WZW) theories. Since tensor product multiplicities correspond to the infinite-level limit of fusion multiplicities, our current efforts are concentrated on incorporating the finite-level dependence into the characterization of the multiplicities in terms of convex polytopes and their discretized volumes. That again relies on our recent studies of three-point correlation functions in WZW theory [7, 8]. We intend to report more on this in the future.

Related in spirit to our approach is the recent work [9] on fusion rules in $SU(N)$ WZW theory. For lower ranks the authors discuss a combinatorial relation between three-point fusion multiplicities and numbers of certain group theoretical orbits. It would be interesting to understand how the results of [9] are related to ours.

Acknowledgments

We thank J Patera for discussions and T Gannon for comments. JR was supported in part by a PIMS Postdoctoral Fellowship and by NSERC and MAW was supported in part by NSERC.

References

- [1] Berenstein A D and Zelevinsky A V 1992 *J. Algebr. Comb.* **1** 7
- [2] Rasmussen J and Walton M A 2000 $su(N)$ tensor product multiplicities and virtual Berenstein–Zelevinsky triangles *Preprint math-ph/0010051*.
- [3] Zelevinsky A 1997 Littlewood–Richardson semigroups *Preprint math.CO/9704228*
- [4] Fulton W 1999 Eigenvalues, invariant factors, highest weights, and Schubert calculus *Preprint math.AG/9908012*
- [5] Gelfand I M and Zelevinsky A 1985 *Group Theoretical Methods in Physics Proc. Third Seminar Yurmala* (Amsterdam: North-Holland)
- [6] Berenstein A and Zelevinsky A 1988 *J. Geom. Phys.* **5** 453
Berenstein A and Zelevinsky A 1999 Tensor product multiplicities, canonical bases and totally positive varieties *Preprint math.RT/9912012*
- [7] Rasmussen J 1999 *Int. J. Mod. Phys. A* **14** 1225
- [8] Rasmussen J and Walton M A On the level-dependence of Wess–Zumino–Witten three-point functions *Preprint hep-th/0105294 (Nucl. Phys. B, at press)*
- [9] Feingold A J and Weiner M D 2000 Type A fusion rules from elementary group theory *Preprint math.QA/0012194*